Title	Cutibacterium acnes-derived extracellular vesicles promote tumor growth in renal cell carcinoma
Author(s)	Jingushi, Kentaro; Kawashima, Atsunari; Tanikawa, Sayaka et al.
Citation	Cancer Science. 2024
Version Type	VoR
URL	https://hdl.handle.net/11094/97094
rights	This article is licensed under a Creative Commons Attribution-NonCommercial 4.0 International License.
Note	

ORIGINAL ARTICLE

Cutibacterium acnes-derived extracellular vesicles promote tumor growth in renal cell carcinoma

Kentaro Jingushi[1] | Atsunari Kawashima[2] | Sayaka Tanikawa[1] | Takuro Saito[3,4] | Akinaru Yamamoto[2] | Toshihiro Uemura[2] | Nesrine Sassi[2] | Yu Ishizuya[2] | Yoshiyuki Yamamoto[2] | Taigo Kato[2] | Koji Hatano[2] | Hiroaki Hase[1] | Norio Nonomura[2] | Kazutake Tsujikawa[1]

[1]Laboratory of Molecular and Cellular Physiology, Graduate School of Pharmaceutical Sciences, Osaka University, Suita, Osaka, Japan

[2]Department of Urology, Graduate School of Medicine, Osaka University, Suita, Japan

[3]Department of Surgery, Graduate School of Medicine, Osaka University, Suita, Osaka, Japan

[4]Department of Clinical Research in Tumor Immunology, Graduate School of Medicine, Osaka University, Suita, Osaka, Japan

Correspondence
Kentaro Jingushi, Laboratory of Molecular and Cellular Physiology, Graduate School of Pharmaceutical Sciences, Osaka University, 1-6 Yamadaoka, Suita, Osaka 565-0871, Japan.
Email: jingushi-kk@phs.osaka-u.ac.jp

Abstract

Bacterial flora are present in various parts of the human body, including the intestine, and are thought to be involved in the etiology of various diseases such as multiple sclerosis, intestinal diseases, cancer, and uterine diseases. In recent years, the presence of bacterial 16S rRNA genes has been revealed in blood, which was previously thought to be a sterile environment, and characteristic blood microbiomes have been detected in various diseases. However, the mechanism and the origin of the bacterial information are unknown. In this study, we performed 16S rRNA metagenomic analysis of bacterial DNA in serum extracellular vesicles from five healthy donors and seven patients with renal cell carcinoma and detected *Cutibacterium acnes* DNA as a characteristic bacterial DNA in the serum extracellular vesicles of patients with renal cell carcinoma. In addition, *C. acnes* DNA was significantly reduced in postoperative serum extracellular vesicles from patients with renal cell carcinoma compared with that in preoperative serum extracellular vesicles from these patients and was also detected in tumor tissue and extracellular vesicles from tumor tissue-associated microbiota, suggesting an association between *C. acnes* extracellular vesicles and renal cell carcinoma. *C. acnes* extracellular vesicles were taken up by renal carcinoma cells to enhance their proliferative potential. *C. acnes* extracellular vesicles also exhibited tumor-promoting activity in a mouse model of renal cancer allografts with enhanced angiogenesis. These results suggest that extracellular vesicles released by *C. acnes* localized in renal cell carcinoma tissues act in a tumor-promoting manner.

KEYWORDS
16S rRNA gene, bacterial DNA, *Cutibacterium acnes*, extracellular vesicles, renal cell carcinoma

1 | INTRODUCTION

Bacterial flora are present in various parts of the human body, including the intestine, and are involved in the etiology of various diseases such as chronic kidney disease,[1] intestinal diseases,[2] and diabetes.[3] The metabolic environment produced by the gut microbiota influences carcinogenesis,[4] cancer progression,[5] and sensitivity to drugs such as immune checkpoint inhibitors in various cancer types, including renal cell carcinoma (RCC).[6–9] In addition, tumor tissues have their own bacterial flora.[10] However, it is unclear how bacteria localized in tumor tissue influence tumor progression.

Blood has long been considered free of microorganisms, and the detection of microorganisms in blood is an indicator of sepsis.[11] In recent years, however, 16S rRNA genes have been detected in "sterile" environments, including blood.[12–14] The presence of bacterial genomic DNA in the bloodstream, characteristic of patients with cancer, may be useful for cancer diagnosis.[15] However, it is unclear whether the information on bacterial flora localized in tumor tissue is reflected in those in the bloodstream.

Extracellular vesicles (EVs) are microparticles released from the domains of eukaryotes, bacteria, and archaea.[16] EVs released by bacteria encapsulate 16S rRNA genes.[17] Information on the characteristic blood EVs-derived bacterial flora has been reported in patients with urothelial carcinoma[18] and in those with RCC.[19] In renal cancer, the blood BTS index (Bacteroidia, TM7-1, and Sphingomonadales) reflects cancer diagnosis, nivolumab drug sensitivity, and the number of infiltrated regulatory T cells (Tregs) in the tumor.[19] However, the mechanism and the origin of the bacterial information are unknown.

To address these gaps, we previously developed a method to collect tissue-exudative EVs (Te-EVs), released from cells and bacteria constituting tumor tissue, by the short-term culture of postoperative resected tissue.[20,21] In the present study, we aimed to establish a noninvasive method for obtaining information on bacteria localized in tumor tissue and to elucidate the effects of tumor tissue-localized bacteria on RCC by analyzing bacterial information in tumor tissue, tumor Te-EVs, and pre- and postoperative serum EVs.

2 | MATERIALS AND METHODS

2.1 | Clinical specimens

Clinical specimens were collected from five healthy donors (HDs) and seven patients with RCC at the Osaka University Hospital (Osaka, Japan). In this study, HDs were defined as those without a current malignant disease or medical history of urinary cancer. Written informed consent was obtained from each patient, and the study was approved by the Ethics Review Board of the Osaka University Medical Hospital (no. 13397-2, no. 14069-3). Clinical and histopathological data related to clinical specimens are presented in Table 1.

2.2 | Isolation of serum and Te-EVs

For serum EV isolation, whole blood samples (2–7 mL) were collected directly into Venoject II tubes (Terumo). Within 3 h of collection, all samples were centrifuged at 4°C 1200 g for 15 min, and supernatants (obtained as serum) were stored at −80°C until analysis. Serum samples were again centrifuged at 18°C 2000 g for 30 min and filtered through a 0.2 μm syringe filter (Kurabo, Osaka, Japan). Thereafter, EVs were isolated from the filtered sera by ultracentrifugation at 4°C 100,000 g for 90 min (SW55 rotor, Beckman Coulter; Optima L-90K, Beckman Coulter) to obtain pellets of EVs. The pellets were then washed with PBS and recovered in PBS as the EV fraction.

For Te-EV isolation, the tissue samples, following excision, were immediately immersed in 4 mL DMEM (FUJIFILM Wako) without FCS and incubated at 37°C for 2 h. The tissue-immersed media were then

TABLE 1 Clinical and histopathological data.

Sample ID	Surgical method	Age	Sex	BMI	pT	cN	cM	Main tumor grade	Histological type
HD1	Laparoscopic donor nephrectomy	66	Male	22.66					
HD2	Laparoscopic donor nephrectomy	71	Female	22.64					
HD3	Laparoscopic donor nephrectomy	47	Female	22.37					
HD4	Laparoscopic donor nephrectomy	70	Male	21.38					
HD5	Laparoscopic donor nephrectomy	73	Female	20.02					
RCC1	CT-guided needle biopsy	76	Female	15.93	1a	0	1	Unknown	Clear cell renal cell carcinoma
RCC2	Laparoscopic nephrectomy	66	Male	20.34	3a	0	0	4	Clear cell renal cell carcinoma
RCC3	Laparoscopic nephrectomy	76	Male	26.81	1a	0	0	2	Clear cell renal cell carcinoma
RCC4	Laparoscopic nephrectomy	61	Male	24.02	1b	0	0	2	Clear cell renal cell carcinoma
RCC5	Laparoscopic nephrectomy	70	Male	19.76	1a	0	0	2	Clear cell renal cell carcinoma
RCC6	Robot-assisted partial nephrectomy	69	Male	20.37	1a	0	0	1	Clear cell renal cell carcinoma
RCC7	Robot-assisted partial nephrectomy	73	Male	22.96	1a	0	0	2	Clear cell renal cell carcinoma

centrifuged at 4°C 2000*g* for 30 min and filtered through a 0.2-μm syringe filter (Kurabo). Thereafter, the supernatants were subjected to ultracentrifugation at 4°C 100,000*g* for 90 min for recovery of EVs using Optima L-90K (Beckman coulter) and SW55Ti rotor (Beckman coulter).

2.3 | Isolation of DNA from EVs and tumor tissues

DNA was isolated from the serum EVs, tumor Te-EVs, *Cutibacterium acnes* EVs, and *Escherichia coli* EVs using the QIAamp® Circulating Nucleic Acid Kit (Qiagen) according to the manufacturer's instructions. Additionally, DNA was isolated from tumor tissues using the DNeasy PowerSoil Pro Kit (Qiagen) according to the manufacturer's protocol. The recovered DNA was assayed using a Qubit dsDNA HS Assay Kit (Thermo Fisher Scientific).

2.4 | 16S Metagenomic sequencing

The PCR-amplified V1–V2 region of the bacterial 16S rRNA gene was sequenced using MiSeq platform (Illumina). PCR was performed using KAPA HiFi™ HS ReadyMix (NIPPON Genetics), with 2.5 ng of starting DNA. PCR was performed for 25 cycles, with each cycle consisting of a denaturation step at 95°C for 15 s, annealing at 63°C for 20 s, and extension at 72°C for 30 s. Each library was prepared according to the "Illumina 16S Metagenomic Sequencing Library Preparation Guide," with a primer set (27Fmod: 5′-TCG GCA GCG TCA GAT GTG TAT AAG AGA CAG AGR GTT TGA TYM TGG CTC AG-3′ and 338R: 5′-GTC TCG TGG GCT CGG AGA TGT GTA TAA GAG ACA GTG CTG CCT CCC GTA GGA GT-3′) targeting the V1–V2 region of the 16S rRNA gene. Thereafter, 251-bp paired-end sequencing of the amplicon was performed on a MiSeq (Illumina) using an MiSeq v2 500 cycle kit (15 cycles each for first and second PCR). The obtained paired-end sequences were merged, filtered, and denoised using DADA2 (https://benjjneb.github.io/dada2/). Taxonomic assignment was performed using the QIIME2 feature classifier plugin on the Greengenes 13_8 database. The bioinformatics pipeline QIIME2 (V.2020.2) was used as the informatics environment for the processing of raw sequencing data. To visualize the positions of each group, the Emperor software tool was used for principal component analysis. Heat tree analysis was conducted using MicrobiomeAnalyst (https://www.microbiomeanalyst.ca).[22] Heat tree analysis utilizes the taxonomic hierarchy to illustrate differences between microbial communities in HDs and RCC patients, as well as in pre- and postsurgical samples, both quantitatively (using median abundance values) and statistically (using nonparametric Wilcoxon rank-sum tests). The image is generated using the web-based platform MicrobiomeAnalyst. The trees are automatically created and arranged in the presence of multiple roots to the taxonomy. Only significant taxon names are labeled on the heat tree ($p < 0.05$). Linear discriminant analysis effect size (LEfSe) was used to elucidate bacterial genus classification taxa that were associated with RCC.[23] LEfSe, an algorithm that is used for discovering

and explaining high-dimensional biomarkers, identifies genomic features that characterize differences between two or more biological conditions (or classes). LEfSe employs Kruskal–Wallis rank-sum test to detect features with significant differential abundance with respect to class labels. This is followed by linear discriminant analysis (LDA) to evaluate the relevance or effect size of differentially abundant features.

2.5 | Bacterial culture and isolation of EVs

The *C. acnes* strain Sijpesteijn, obtained from ATCC (ATCC 49949), was cultured in modified Gifu anaerobic medium (GAM) broth, (Nissui Pharmaceutical) at 37°C under anaerobic conditions. The *E. coli* strain (Migula 1895) Castellani and Chalmers 1919, obtained from the National Institute of Technology and Evaluation, Biological Resource Center (NBRC, NBRC 3301), was cultured in modified GAM broth at 37°C under anaerobic conditions.

For *C. acnes* EV isolation, *C. acnes* was cultured at 35°C for 3 days in modified GAM broth, and then subjected to centrifugation at 4°C for 30 min at 2000*g*. The supernatant was passed through a 0.2-μm syringe filter (Kurabo) before being subjected to EV isolation. The filtered supernatant was centrifuged at 4°C at 100,000*g* for 90 min (Optima L-90K; SW28 rotor; Beckman Coulter) to obtain pellets of EVs. Thereafter, the pellets were washed with PBS and recovered in PBS to obtain the EV fraction.

For *E. coli* EV isolation, *E. coli* was cultured at 37°C for 18 h at 250 rpm with shaking and then subjected to centrifugation at 4°C for 30 min at 2000*g*. The supernatant was passed through a 0.2 μm syringe filter (Kurabo) before being subjected to EV isolation. The filtered supernatant was centrifuged at 4°C at 100,000*g* for 90 min (Optima L-90K; SW28 rotor; Beckman Coulter) to obtain pellets of EVs. Thereafter, the pellets were washed with PBS and recovered in PBS to obtain the EV fraction.

As with the bacterial culture supernatant, the GAM medium itself was ultracentrifuged, suspended in PBS, and used as a negative control.

2.6 | Amplification of 16S rRNA gene from *C. acnes* EVs

For DNA isolation, *C. acnes* EVs were first treated with recombinant DNase I (TaKaRa Bio) according to the manufacturer's instructions. Bacterial DNA of *C. acnes* was detected with a primer set (PAS9: 5′-CCC TGC TTT TGT GGG GTG-3′ and PAS11: 5′-CGA CCC CAA AAG AGG GAC-3′) targeting the 16S rRNA gene of *C. acnes*.[24] PCR was performed using KAPA HiFi™ HS ReadyMix (NIPPON Genetics) with 2.5 ng of starting DNA. PCR was performed for 25 cycles, with each cycle consisting of a denaturation step at 95°C for 15 s, annealing at 63°C for 20 s, and extension at 72°C for 30 s. Amplicons were resolved by agarose gel electrophoresis and detected using SAFELOOK™ Green Nucleic Acid Stain (FUJIFILM Wako).

2.7 | Transmission electron microscopy (TEM) of EVs

Transmission electron microscopy was performed according to the method described by Cecilia et al.[25] Briefly, EV samples (1 μg) were placed on a Formvar carbon-coated nickel grid for 1 h, fixed with 2% paraformaldehyde, and observed using a transmission electron microscope (HT7800; Hitachi).

2.8 | Extracellular vesicle nanoparticle measurement

The size and concentration of EVs were determined using qNano Gold with NP150 nanopores, according to the manufacturer's instructions (Izon Science Ltd.). All EV samples and calibration particles (Izon Science Ltd.) were measured at 47.0 mm stretch and 0.5 kPa, with a voltage of 0.5–0.8 V. Data were analyzed using the Izon Control Suite Software (V3.3.2.2001).

2.9 | Culture of renal carcinoma (RC) cells

The human RCC cell lines 786-O and Caki-2 and the mouse RCC cell line RenCa, all obtained from the ATCC, were cultured in RPMI1640 medium (Wako) supplemented with 10% FBS (Thermo Fisher Scientific) and 100 μg/mL kanamycin (Wako).

2.10 | Extracellular vesicle incorporation assay

Caki-2 cells, 786-O cells, and RenCa cells were precultured in a 24-well plate (5×10^4 cells/well) and incubated with EVs (5×10^8 particles/well) stained with PKH67 Green Fluorescent Cell Linker Kit (Sigma-Aldrich) for 24 h. Thereafter, the cells were analyzed using MACSQuant X (Miltenyi Biotec) or a confocal microscope Bio-Zero (KEYENCE). Data were analyzed using the MACSQuantify software (Miltenyi Biotec).

2.11 | Water-soluble tetrazolium salt-8 (WST-8) cell proliferation assay

Cell proliferation was examined by WST-8 assay. Caki-2 cells, 786-O cells, and RenCa cells were seeded in a 96-well plate (0.25×10^3 cells/well). After 24 h, cells were incubated with EVs (1×10^8 particles/well) for the indicated time. After incubation for 2 h with the WST-8 reagent (Dojindo) at 37°C and 5% CO_2, the absorbance was measured at a wavelength of 450/630 nm (Ex/Em).

2.12 | In vivo experiments

Five-week-old male BALB/c mice were purchased from Japan SLC, Inc. The animals were housed under 12-h light–dark cycles at 22°C–24°C. RenCa cells were adjusted to a concentration of 1.0×10^6 cells suspended in 50 μL serum-free RPMI1640. The cell suspensions with 50 mL matrigel (Corning) were then injected subcutaneously into the right flanks of the mice. When the tumor diameter reached 100 mm³, PKH26-labeled *C. acnes* or *E. coli* EVs (1.0×10^{10} particles suspended in 100 μL PBS) were administered intraperitoneally to each mouse. PKH-26-labeled PBS was used as a negative control. Tumors were resected 30 min after EV injection, and frozen tumor sections were analyzed using SLIDEVIEW VS200 (OLYMPUS).

For the assessment of *C. acnes* and *E. coli* EVs on the tumor growth, when the tumor diameter reached 100 mm³, *C. acnes* or *E. coli* EVs (1.0×10^{10} particles suspended in 100 μL PBS) were administered intraperitoneally to each mouse. After 10 days following EV injection, tumors were resected, and frozen tumor tissues were subjected to immunohistochemistry using Ki67 (1:200; ab16667; Abcam), CD31 (1:500; #77699; Cell Signaling Technology), or isotype control IgG (ab172730; Abcam) antibodies and EnVision+ Detection System (DAKO), according to the manufacturer's instructions. Using the image analysis software HALO with AI function, the number of positive cells in the immunohistochemically stained images, captured with the Research Slide Scanner VS200, was measured. Positive cells were classified into three levels (strong, medium, weak) according to staining intensity. The classification criteria were: Ki67; strong: >0.33, medium: 0.11–0.33, weak: 0.02–0.10, with the maximum staining intensity set at 1. All animal experiments were approved by the Animal Experimentation Committee of the Graduate School of Pharmaceutical Science at Osaka University (Douyaku R04-10).

2.13 | Statistical analyses

Statistical analyses and visualization quantification were performed using GraphPad Prism software (GraphPad Prism 6.0, GraphPad software). Differences between values were statistically analyzed using the Mann–Whitney U test. A p-value < 0.05 was considered statistically significant.

3 | RESULTS

3.1 | *Cutibacterium acnes* genomic DNA is enriched in serum EVs of patients with RCC

Bacterial genomic DNA in serum EVs obtained from five HDs and seven patients with RCC were analyzed by 16S rRNA metagenomic analysis (Figure 1A). The α-diversity and observed operational taxonomic units (OTUs) did not differ significantly between HD and patients with RCC (Figure 1B–E). Heat tree (Figure 1F) and LEfSe (Figure 1G) analyses showed the phylogenetic composition of common bacterial taxa at the species level, revealing the abundance of *C. acnes* in serum EVs from patients with RCC compared with that in serum EVs from HD (Figure 1H). DNA was recovered from serum EVs of preoperative and postoperative patients with RCC, and subjected to 16S rRNA metagenomic analysis (Figure 2A). The
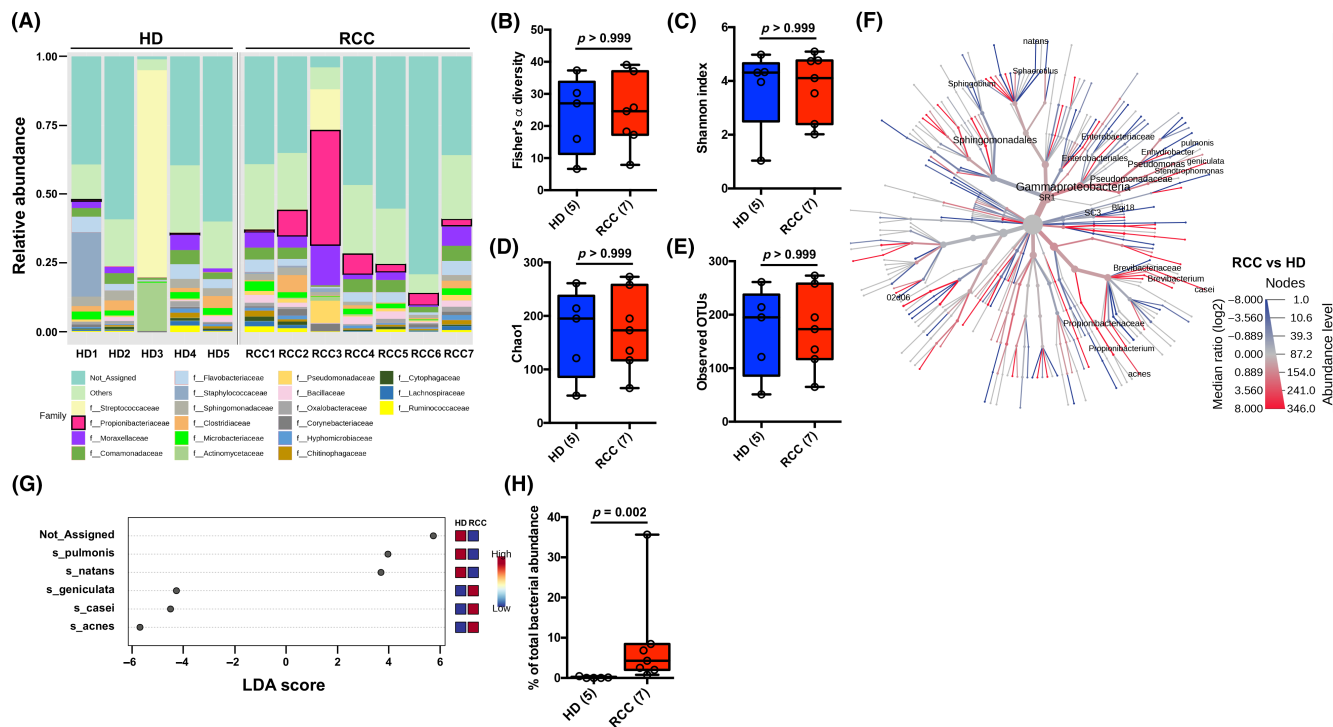
FIGURE 1 *Cutibacterium acnes* genomic DNA is enriched in renal cell carcinoma (RCC) patient serum extracellular vesicles (EVs). (A) Taxa bar plots of healthy donors (HD) and RCC serum EVs. Results of diversity analysis of Fisher's α diversity (B), Shannon index (C), and Chao1 (D) of HD and RCC serum EVs. (E) Observed operational taxonomic units (OTUs). Number of the samples is given in parentheses. (F) Heat tree analysis leverages the hierarchical structure of taxonomic classifications to quantitatively (using median abundance) and statistically (using non-parametric Wilcoxon rank-sum test) depict taxonomic differences between microbial communities in RCC and HD serum EVs (RCC vs. HD). (G) Distinctive bacterial species between RCC and HD and the percentage of species abundance of each species. LDA: linear discriminant analysis. (H) Percentage of *C. acnes* abundance. Number of the samples is given in parentheses. Mann–Whitney test (two tailed).

α-diversity and observed OTUs were significantly increased after surgery compared with those prior to surgery (Figure 2B–E). Heat tree (Figure 2F) and LEfSe (Figure 2G) analyses revealed that the percentage of *C. acnes* decreased significantly after surgery compared with that prior to surgery (Figure 2H). In contrast, analysis of the sera themselves showed no significant difference in *C. acnes* bacterial DNA abundance between preoperative and postoperative patients with RCC (Figure 2I). To verify the origin of the *C. acnes* bacterial DNA detected in serum EVs, DNA was recovered from tumor tissue and tumor Te-EVs of the same patient corresponding to the serum samples and subjected to 16S rRNA metagenomic analysis. The results revealed the presence of *C. acnes* bacterial DNA in tumor tissue and tumor Te-EVs (Figure S1), suggesting the association between *C. acnes* and RCC.

## 3.2 | *Cutibacterium acnes*-derived EVs promote the proliferation of RC cells

To clarify whether the bacterial DNA of *C. acnes* detected in serum EVs from patients with RCC was derived from EVs released by *C. acnes*, *C. acnes* was cultured and EVs were recovered (Figure 3A–C). DNA was isolated from *C. acnes* EVs after DNase I treatment, and PCR was performed using primers specific for the *C. acnes* 16S RNA

gene. The results revealed that the *C. acnes* 16S rRNA gene was internalized in *C. acnes* EVs (Figure 3D), suggesting that the *C. acnes* bacterial DNA detected in serum EVs from patients with RCC was derived from EVs released by *C. acnes*.

To analyze the effect of *C. acnes* EVs on RC cells, we first performed uptake assays on RC cell lines (Caki-2, 786-O, and RenCa cells). In addition, EVs recovered from the culture medium of *E. coli*, one of the typical commensal bacteria, were used as control bacterial EVs (Figure S2A,B). The results showed that both *C. acnes* and *E. coli* EVs were incorporated in all RC cell lines (Figure 4A–D); however, only *C. acnes* EVs had a promoting effect on the cell growth of RC cells (Figure 4E–J).

## 3.3 | *Cutibacterium acnes*-derived EVs promote tumor growth in vivo

We administered both *C. acnes* and *E. coli* EVs intraperitoneally to a mouse model of tumor-bearing carcinoma using RenCa cells and examined their effects on tumor growth. First, we tested whether intraperitoneally administered bacterial EVs could reach tumors. The results showed that both *C. acnes* and *E. coli* EVs can reach tumors via intraperitoneal administration (Figure 5A–C). Tumor growth was enhanced by *C. acnes* EV administration (Figure 5D).
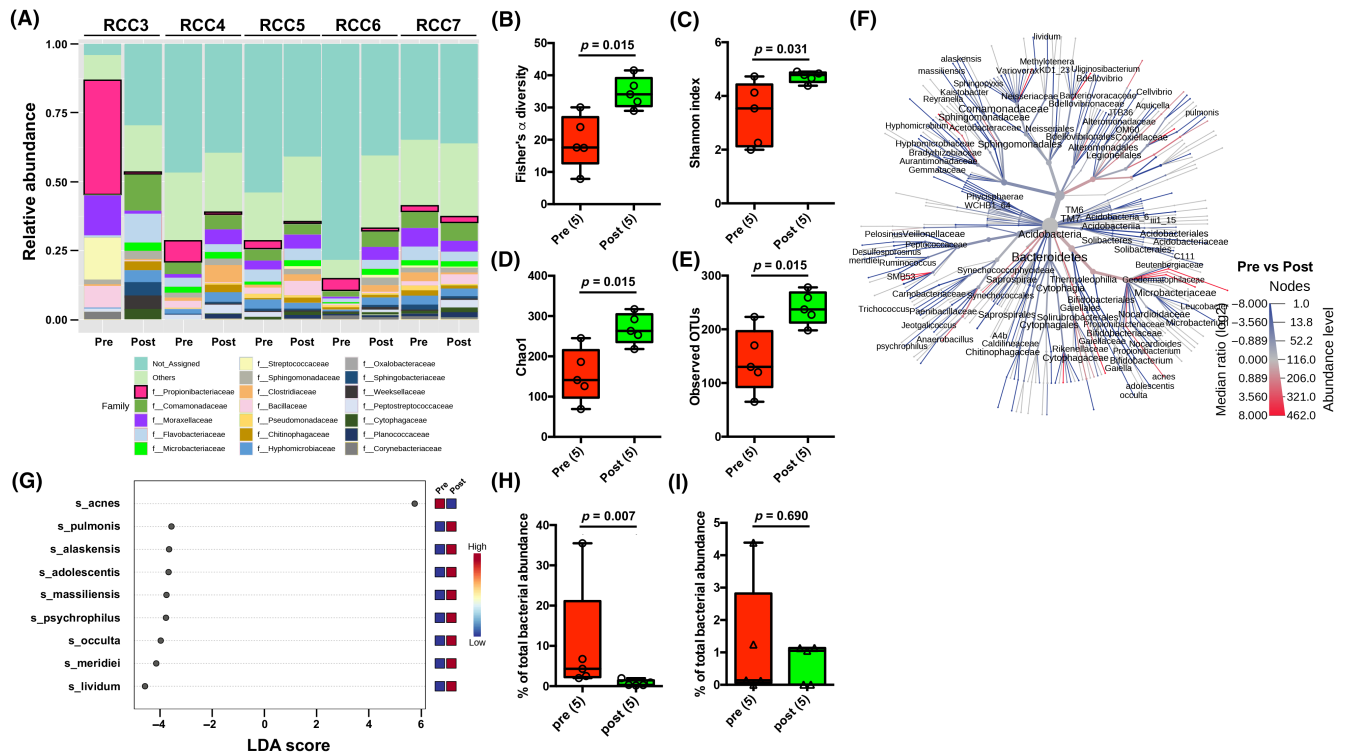
FIGURE 2 16S ribosomal RNA metagenomic analysis of pre- and postoperative serum extracellular vesicles (EVs). (A) Taxa bar plots of pre- and postoperative serum EVs. Results of diversity analysis of Fisher's α diversity (B), Shannon index (C), and Chao1 (D) of pre- and postoperative serum EVs. (E) Observed operational taxonomic units (OTUs). Number of the samples is given in parentheses. (F) Heat tree analysis leverages the hierarchical structure of taxonomic classifications to quantitatively (using median abundance) and statistically (using nonparametric Wilcoxon rank-sum test) depict taxonomic differences between microbial communities in pre- and postoperative serum EVs (pre vs. post). (G) Distinctive bacterial species between pre- and postoperative serum EVs and the percentage of species abundance of each species. LDA: linear discriminant analysis. Percentage of *C. acnes* abundance in serum EVs (H) and serum (I). Number of the samples is given in parentheses. Mann–Whitney test (two tailed).
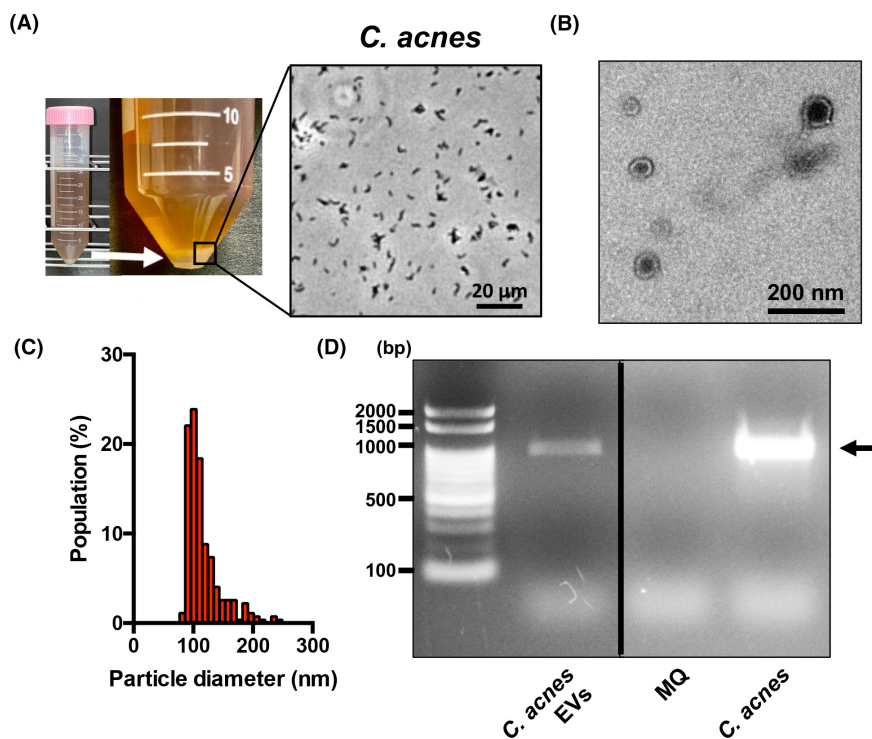
FIGURE 3 *Cutibacterium acnes* releases extracellular vesicles (EVs) with its genomic DNA. (A) A representative image of *C. acnes* culture. (B) Electron microscopic image of *C. acnes* EVs. Black bars indicate 200nm. A representative image of three independent experiments is shown. (C) Nanoparticle tracking analysis of *C. acnes* EVs. A representative image of three independent experiments is shown. (D) PCR targeting 16S rRNA gene of *C. acnes* in *C. acnes* EVs. Figures are representative of three independent results. Black arrow indicates 946-bp amplified region of *C. acnes* 16S rRNA gene. MQ: Milli-Q water.
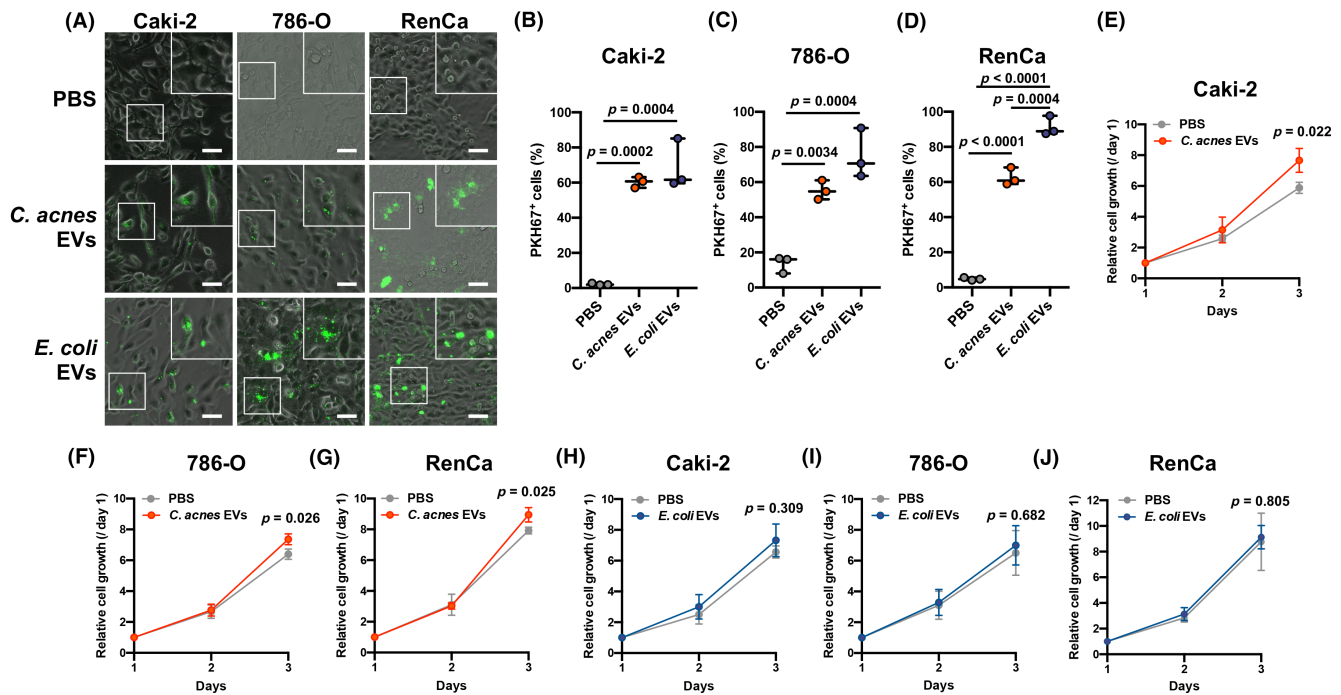
FIGURE 4 _Cutibacterium acnes_ extracellular vesicles (EVs) promote proliferation of renal carcinoma cells. (A) Confocal microscopy analyses of renal cancer cells incubated with PKH67-labeled _C. acnes_ EVs or _E. coli_ EVs for 24 h. White bars indicate 50 μm. A representative image of three independent experiments is shown. (B–D) Flow cytometry analyses of renal cancer cells: (B) Caki-2, (C) 786-O, and (D) RenCa. Cells were incubated with PKH67-labeled _C. acnes_ EVs or _E. coli_ EVs for 24 h. One-way ANOVA test (post-hoc Tukey). (E–G) Proliferation assay of renal cancer cells: (E) Caki-2, (F) 786-O, and (G) RenCa. Cells were incubated with _C. acnes_ EVs. Unpaired _t_-test. (H–J) Proliferation assay of renal cancer cells: (H) Caki-2, (I) 786-O, and (J) RenCa. Cells were incubated with _E. coli_ EVs. Unpaired _t_-test.

Immunohistochemical staining was performed using antibodies against the proliferation marker Ki67 and the vascular endothelial cell marker CD31 (Figure 5E). The results showed that the percentage of Ki67-overexpressing cells and CD31-positive cells in the tumor were markedly increased by _C. acnes_ EVs (Figure 5F–I). In contrast, _E. coli_ EVs showed no significant effect on tumor growth (Figure 5J) and had no effect on the percentage of cells positive for Ki67 or CD31 (Figure 5K–O). These results indicated that _C. acnes_ EVs had a tumor-promoting effect on RC.

4 | DISCUSSION

Cutibacterium acnes localizes to tumor tissues and acts in a tumor-promoting manner in various cancer types. In gastric cancer, _C. acnes_ contributes to tumor progression by promoting the differentiation of macrophages into M2 macrophages[26]; whereas in ovarian cancer, _C. acnes_ acts in a tumor-promoting manner by activating the Hedgehog signaling pathway.[27] In thyroid cancer, the higher the amount of _C. acnes_, the higher the number of Treg infiltrates and the lower the intratumor immune activity.[28] In contrast, EVs released by _C. acnes_, and their effects on cancer are unknown. In this study, we found that the bacterial DNA of _C. acnes_ is a characteristic bacterial DNA present in serum EVs from patients with RCC. Moreover, _C. acnes_ bacterial DNA was detected not only in RC tumor tissue but also in

RC tumor Te-EVs, suggesting that the EVs released by _C. acnes_ and localized in RC tumor tissue may be working in a tumor-promoting manner.

Cutibacterium acnes EVs were found to be taken up by RC cell lines and to enhance their proliferative potential. _C. acnes_ EVs were also shown to act in a tumor-promoting manner in RC tumor-bearing mice. However, the mechanism by which _C. acnes_ EVs promote the growth of RC cells remains unclear. _C. acnes_ EVs promote the MAPK and NF-κB signaling pathways via Toll-like receptor 2 (TLR2) in keratinocytes[29]; therefore, it is possible that _C. acnes_ EVs promote the proliferation of RC cells via these signals. Further studies on the content of _C. acnes_ EVs will help to elucidate the mechanism by which they act in a tumor-promoting manner.

Our data showed that the abundances of several bacteria taxa, including _Bifidobacterium adolescentis_[30] and _Bariatricus massiliensis_,[31] which have been identified as gut bacteria, were upregulated in the serum EVs obtained from RCC patients after surgery. Surgery can alter the composition of the gut microbiome in the gastrointestinal tract.[32] Therefore, surgery might also impact the gut microbiome composition in the kidney, and some of these changes could be reflected in the blood after surgery.

In the present study, upregulated CD31 expression in tumors following treatment with _C. acnes_ EVs suggested that _C. acnes_ EVs may also contribute to angiogenesis by increasing vascular endothelial cells in the tumor. Cancer cells induce angiogenesis by releasing
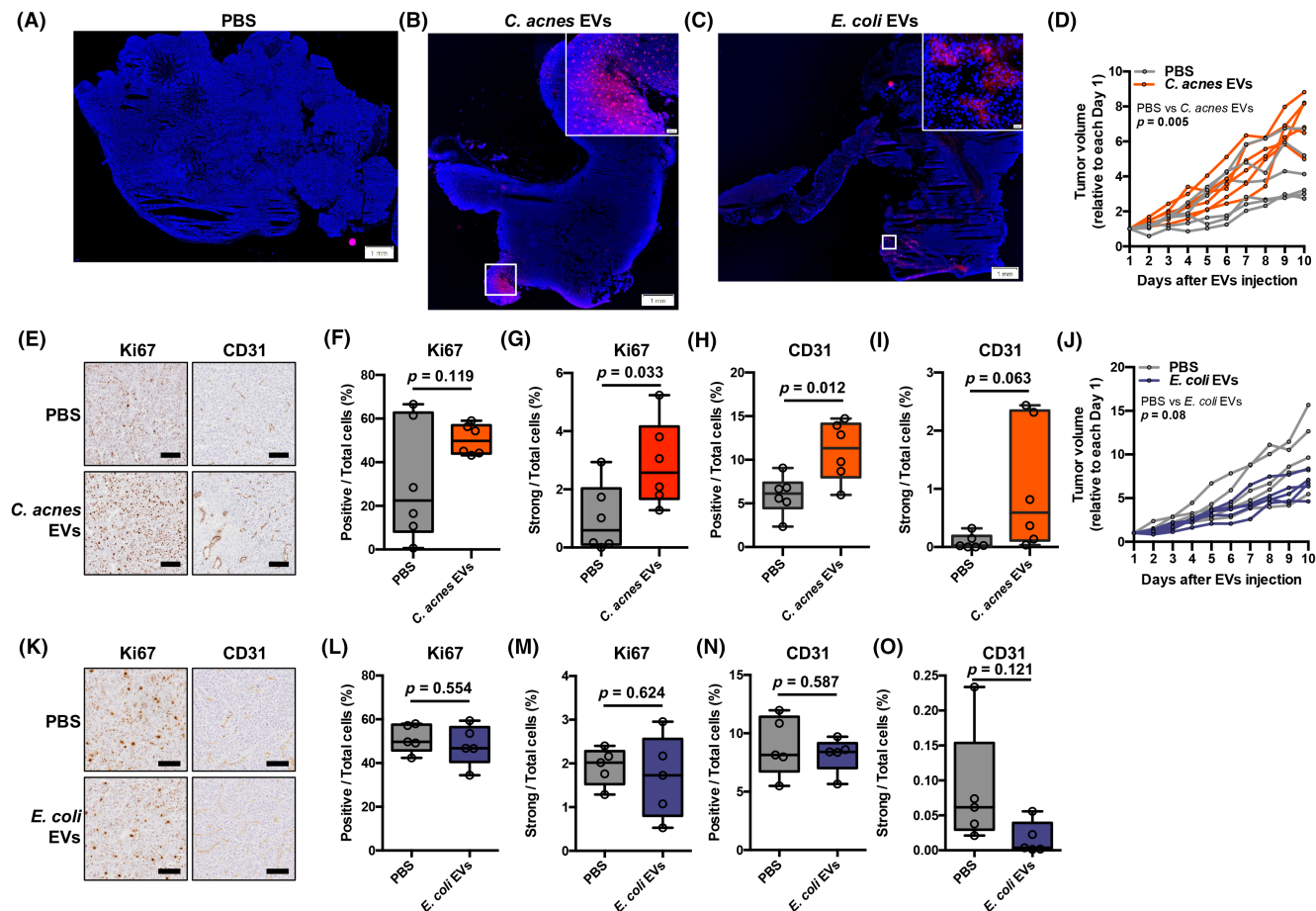
FIGURE 5 *Cutibacterium acnes* extracellular vesicles (EVs) promote renal cell carcinoma tumor growth in vivo. PKH26-labeled PBS (A), *C. acnes* EVs (B), or *E. coli* EVs (C) were intraperitoneally administered to mice with RenCa tumors and subjected to immunofluorescence analysis. A representative image of two independent experiments is shown. (D) The effect of *C. acnes* EVs on RenCa cell tumor growth. Unpaired *t*-test. (E) Immunohistochemistry (IHC) of RenCa cell tumor using anti-Ki67 and anti-CD31 antibodies. Figure shows a representative image of IHC. Percentage of Ki67-positive (F) and CD31-positive (H) cells and percentage of Ki67 (G) and CD31 (I) highly positive cells. Unpaired *t*-test. (J) The effect of *E. coli* EVs on RenCa cell tumor growth. (K) IHC of RenCa cell tumor using anti-Ki67 and anti-CD31 antibodies. Figure shows a representative image of IHC. Percentage of Ki67-positive (L) and CD31-positive (N) cells and percentage of Ki67 (M) and CD31 (O) highly positive cells.

VEGF[33]; in contrast, in thyroid and prostate cancers, *C. acnes* present in cancer tissues increases the number of Treg infiltrates.[28,34] Furthermore, Tregs contribute to angiogenesis by enhancing the production of VEGF.[35] Thus, *C. acnes* EVs may contribute to the increase in vascular endothelial cells either by promoting the proliferation of RC cells or by increasing the number of Treg infiltrates in the tumor.

There are several limitations to this study. First, it is based solely on a retrospective analysis with a small sample size and needs to be validated on multiple samples. Second, apart from that on vascular endothelial cells, the effect of *C. acnes* EVs on immune cells and other stromal cells in tumors is unknown. Third, the physical presence of *C. acnes* in the RC tissue is unclear. Adhesive Flp pili encoded by the tight adherence locus can promote colonization of *C. acnes* in prostate tumor tissue,[36] suggesting that the increase of *C. acnes* in RCC tissue may also be promoted by these cilia. Clear-cell RCC, which accounts for about 70%–85% of RCCs, is characterized

by the high lipid content of its cells[37] and a hypoxic environment in the cancerous tissue.[38] Culturing *C. acnes* in a lipid-rich hypoxic environment enhances short-chain fatty acid- and TLR2-mediated IL-6, IL-8, and TNFα cytokine production in human keratinocytes,[29] which promotes RC development.[39–41] Thus, although their underlying mechanism is unknown, it is possible that the RC tumor microenvironment induces the tumor-promoting function of *C. acnes*.

AUTHOR CONTRIBUTIONS

Koji Hatano: Investigation; methodology; resources; validation; writing – review and editing. **Taigo Kato:** Investigation; methodology; resources; validation; writing – review and editing. **Yoshiyuki Yamamoto:** Investigation; methodology; resources; validation; writing – review and editing. **Hiroaki Hase:** Investigation; methodology; resources; validation; writing – review and editing. **Kazutake Tsujikawa:** Investigation; methodology; resources; supervision; validation; writing – review and editing. **Norio Nonomura:** Investigation;

CONFLICT OF INTEREST STATEMENT

The authors have no conflict of interest.

DISCLOSURE

Dr. Norio Nonomura is an associate editor of *Cancer Science*.

ETHICS STATEMENTS

Approval of the research protocol by an Institutional Reviewer Board: The study was approved by the Ethics Review Board of the Osaka University Medical Hospital (no. 13397-2, no. 14069-3).
Registry and the Registration No. of the study/trial: N/A.
Informed Consent: Written informed consent was obtained from each patient.
Animal Studies: All animal experiments were approved by the Animal Experimentation Committee of the Graduate School of Pharmaceutical Science at Osaka University (Douyaku R04-10).

ORCID

Kentaro Jingushi https://orcid.org/0000-0002-2274-4962
Atsunari Kawashima https://orcid.org/0000-0001-9369-4264
Takuro Saito https://orcid.org/0000-0002-1733-5064
Taigo Kato https://orcid.org/0000-0002-8681-1407
Norio Nonomura https://orcid.org/0000-0002-6522-6233

REFERENCES

1. Meijers B, Evenepoel P, Anders H. Intestinal microbiome and fitness in kidney disease. *Nat Rev Nephrol.* 2019;15(9):531-545. doi:10.1038/s41581-019-0172-1
2. Vijay A, Valdes AM. Role of the gut microbiome in chronic diseases: a narrative review. *Eur J Clin Nutr.* 2022;76(4):489-501. doi:10.1038/s41430-021-00991-6
3. Crudele L, Gadaleta RM, Cariello M, Moschetta A. Gut microbiota in the pathogenesis and therapeutic approaches of diabetes. *EBioMedicine.* 2023;97:104821. doi:10.1016/j.ebiom.2023.104821
4. Saito T, Nishikawa H, Wada H, et al. Two FOXP3$^+$CD4$^+$ T cell subpopulations distinctly control the prognosis of colorectal cancers. *Nat Med.* 2016;22(6):679-684. doi:10.1038/nm.4086
5. Matsushita M, Fujita K, Hayashi T, et al. Gut microbiota-derived short-chain fatty acids promote prostate cancer growth via IGF1 signaling. *Cancer Res.* 2021;81(15):4014-4026. doi:10.1158/0008-5472.CAN-20-4090
6. Hopkins AM, Kichenadasse G, Karapetis CS, Rowland A, Sorich MJ. Concomitant antibiotic use and survival in urothelial carcinoma treated with atezolizumab. *Eur Urol.* 2020;78(4):540-543. doi:10.1016/j.eururo.2020.06.061
7. Mager LF, Burkhard R, Pett N, et al. Microbiome-derived inosine modulates response to checkpoint inhibitor immunotherapy. *Science.* 2020;369(6510):1481-1489. doi:10.1126/science.abc3421
8. Pederzoli F, Bandini M, Raggi D, et al. Is there a detrimental effect of antibiotic therapy in patients with muscle-invasive bladder cancer treated with neoadjuvant pembrolizumab? *Eur Urol.* 2021;80(3):319-322. doi:10.1016/j.eururo.2021.05.018
9. Salgia NJ, Bergerot PG, Maia MC, et al. Stool microbiome profiling of patients with metastatic renal cell carcinoma receiving anti-PD-1 immune checkpoint inhibitors. *Eur Urol.* 2020;78(4):498-502. doi:10.1016/j.eururo.2020.07.011
10. Nejman D, Livyatan I, Fuks G, et al. The human tumor microbiome is composed of tumor type-specific intracellular bacteria. *Science.* 2020;368(6494):973-980. doi:10.1126/science.aay9189
11. Wiersinga WJ, Poll T. Immunopathophysiology of human sepsis. *EBioMedicine.* 2022;86:104363. doi:10.1016/j.ebiom.2022.104363
12. Nikkari S, McLaughlin IJ, Bi W, Dodge DE, Relman DA. Does blood of healthy subjects contain bacterial ribosomal DNA? *J Clin Microbiol.* 2001;39(5):1956-1959. doi:10.1128/JCM.39.5.1956-1959.2001
13. Dinakaran V, Rathinavel A, Pushpanathan M, Sivakumar R, Gunasekaran P, Rajendhran J. Elevated levels of circulating DNA in cardiovascular disease patients: metagenomic profiling of microbiome in the circulation. *PLoS One.* 2014;9(8):e105221. doi:10.1371/journal.pone.0105221
14. Lelouvier B, Servant F, Païssé S, et al. Changes in blood microbiota profiles associated with liver fibrosis in obese patients: a pilot analysis. *Hepatology.* 2016;64(6):2015-2027. doi:10.1002/hep.28829
15. Poore GD, Kopylova E, Zhu Q, et al. Microbiome analyses of blood and tissues suggest cancer diagnostic approach. *Nature.* 2020;579(7800):567-574. doi:10.1038/s41586-020-2095-1
16. Kalluri R, LeBleu VS. The biology, function, and biomedical applications of exosomes. *Science.* 2020;367(6478):eaau6977. doi:10.1126/science.aau697
17. Kang C, Ban M, Choi E, et al. Extracellular vesicles derived from gut microbiota, especially Akkermansia muciniphila, protect the progression of dextran sulfate sodium-induced colitis. *PLoS One.* 2013;8(10):e76520. doi:10.1371/journal.pone.0076520
18. Jingushi K, Kawashima A, Saito T, et al. Circulating extracellular vesicles carrying firmicutes reflective of the local immune status may predict clinical response to pembrolizumab in urothelial carcinoma patients. *Cancer Immunol Immunother.* 2022;71(12):2999-3011. doi:10.1007/s00262-022-03213-5

19. Uemura T, Kawashima A, Jingushi K, et al. Bacteria-derived DNA in serum extracellular vesicles are biomarkers for renal cell carcinoma. *Heliyon*. 2023;9(9):e19800. doi:10.1016/j.heliyon.2023.e19800

20. Jingushi K, Uemura M, Ohnishi N, et al. Extracellular vesicles isolated from human renal cell carcinoma tissues disrupt vascular endothelial cell morphology via azurocidin. *Int J Cancer*. 2018;142(3):607-617. doi:10.1002/ijc.31080

21. Tomiyama E, Matsuzaki K, Fujita K, et al. Proteomic analysis of urinary and tissue-exudative extracellular vesicles to discover novel bladder cancer biomarkers. *Cancer Sci*. 2021;112(5):2033-2045. doi:10.1111/cas.14881

22. Lu Y, Zhou G, Ewald J, Pang Z, Shiri T, Xia J. MicrobiomeAnalyst 2.0: comprehensive statistical, functional and integrative analysis of microbiome data. *Nucleic Acids Res*. 2023;51(W1):W310-W318. doi:10.1093/nar/gkad407

23. Segata N, Izard J, Waldron L, et al. Metagenomic biomarker discovery and explanation. *Genome Biol*. 2011;12(6):R60. doi:10.1186/gb-2011-12-6-r60

24. Nakamura M, Kametani I, Higaki S, Yamagishi T. Identification of Propionibacterium acnes by polymerase chain reaction for amplification of 16S ribosomal RNA and lipase genes. *Anaerobe*. 2003;9(1):5-10. doi:10.1016/S1075-9964(03)00061-1

25. Lässer C, Eldh M, Lötvall J. Isolation and characterization of RNA-containing exosomes. *J Vis Exp*. 2012;59:e3037. doi:10.3791/3037

26. Li Q, Wu W, Gong D, Shang R, Wang J, Yu H. Propionibacterium acnes overabundance in gastric cancer promote M2 polarization of macrophages via a TLR4/PI3K/Akt signaling. *Gastric Cancer*. 2021;24(6):1242-1253. doi:10.1007/s10120-021-01202-8

27. Huang Q, Wei X, Li W, et al. Endogenous *Propionibacterium acnes* promotes ovarian cancer progression via regulating hedgehog signalling pathway. *Cancers (Basel)*. 2022;14(21):5178. doi:10.3390/cancers14215178

28. Trivedi V, Noronha V, Sreekanthreddy P, et al. Association of Cutibacterium acnes with human thyroid cancer. *Front Endocrinol (Lausanne)*. 2023;14:1152514. doi:10.3389/fendo.2023.1152514

29. Choi E, Lee HG, Bae I, et al. Propionibacterium acnes-derived extracellular vesicles promote acne-like phenotypes in human epidermis. *J Invest Dermatol*. 2018;138(6):1371-1379. doi:10.1016/j.jid.2018.01.007

30. Duranti S, Ruiz L, Lugli GA, et al. Bifidobacterium adolescentis as a key member of the human gut microbiota in the production of GABA. *Sci Rep*. 2020;10(1):14112. doi:10.1038/s41598-020-70986-z

31. Bessis S, Amadou T, Dubourg G, Raoult D, Fournier PE. "Bariatricus massiliensis" as a new bacterial species from human gut microbiota. *New Microbes New Infect*. 2016;12:54-55. doi:10.1016/j.nmni.2016.04.003

32. Tsigalou C, Paraschaki A, Bragazzi NL, et al. Alterations of gut microbiome following gastrointestinal surgical procedures and their potential complications. *Front Cell Infect Microbiol*. 2023;13:1191126. doi:10.3389/fcimb.2023.1191126

33. Xu S, Zhang H, Chong Y, Guan B, Guo P. YAP promotes VEGFA expression and tumor angiogenesis though Gli2 in human renal cell carcinoma. *Arch Med Res*. 2019;50(4):225-233. doi:10.1016/j.arcmed.2019.08.010

34. Davidsson S, Carlsson J, Greenberg L, Wijkander J, Söderquist B, Erlandsson A. *Cutibacterium acnes* induces the expression of immunosuppressive genes in macrophages and is associated with an increase of regulatory T-cells in prostate cancer. *Microbiol Spectr*. 2021;9(3):e0149721. doi:10.1128/spectrum.01497-21

35. Facciabene A, Peng X, Hagemann IS, et al. Tumour hypoxia promotes tolerance and angiogenesis via CCL28 and T(reg) cells. *Nature*. 2011;475(7355):226-230. doi:10.1038/nature10169

36. Davidsson S, Carlsson J, Mölling P, et al. Prevalence of Flp pili-encoding plasmids in Cutibacterium acnes isolates obtained from prostatic tissue. *Front Microbiol*. 2017;8:2241. doi:10.3389/fmicb.2017.02241

37. Tan SK, Welford SM. Lipid in renal carcinoma: queen bee to target? *Trends Cancer*. 2020;6(6):448-450. doi:10.1016/j.trecan.2020.02.017

38. Sebestyén A, Kopper L, Dankó T, Tímár J. Hypoxia signaling in cancer: from basics to clinical practice. *Pathol Oncol Res*. 2021;27:1609802. doi:10.3389/pore.2021.1609802

39. Kamińska K, Czarnecka AM, Escudier B, Lian F, Szczylik C. Interleukin-6 as an emerging regulator of renal cell cancer. *Urol Oncol*. 2015;33(11):476-485. doi:10.1016/j.urolonc.2015.07.010

40. Rizzo M, Varnier L, Pezzicoli G, Pirovano M, Cosmai L, Porta C. IL-8 and its role as a potential biomarker of resistance to anti-angiogenic agents and immune checkpoint inhibitors in metastatic renal cell carcinoma. *Front Oncol*. 2022;12:990568. doi:10.3389/fonc.2022.990568

41. Shi J, Wang K, Xiong Z, et al. Impact of inflammation and immunotherapy in renal cell carcinoma. *Oncol Lett*. 2020;20(5):272. doi:10.3892/ol.2020.12135

SUPPORTING INFORMATION

Additional supporting information can be found online in the Supporting Information section at the end of this article.